SUPPLEMENTARY DISCUSSION

False negative results in the primary screen

To elucidate the possible limitations of the assay, we further analyzed the four cases where we did not identify the primary target of the inhibitor (false negative results). These were the EPHA2 inhibitor HG-6-64-1, the covalent EGFR inhibitor afatinib, the allosteric IGF1R inhibitor I-OMe-AG538[1] and the allosteric IKKβ inhibitor BMS-345541.

Two of these cases were false negatives only in the primary assay. In the primary screen, EPHA2/CDC37 interaction was marginally affected by HG-6-64-1 (**Supplementary Table 2**), but the change was not statistically significant. In a re-test with several concentrations of the inhibitor, however, EPHA2 was displaced from CDC37 with an EC50 of 38 nM (**Supplementary Figure 13**). EPHA2 autophosphorylation was also potently inhibited by the compound (**Supplementary Figure 13**). Similarly, mutant EGFR (L858R) did not pass the statistical cutoff in the primary screen, although its interaction with CDC37 was clearly affected (**Supplementary Table 2**). However, follow-up experiments showed that afatinib potently inhibited EGFR L858R autophosphorylation and affected the EGFR L858R/CDC37 interaction with an EC50 of 4 nM (**Supplementary Figure 13**). Thus, these were false negative results in the primary screen; increasing the number of assay replicates would minimize such cases.

We similarly re-tested IGF1R with multiple concentrations of I-OMe-AG538, a substrate-competitive inhibitor. The inhibitor did not disrupt the IGF1R/CDC37 interaction even at high concentrations (data not shown). Interestingly, autophosphorylation of IGF1R was only slightly inhibited by high concentrations of IGF1R (**Supplementary Figure 13**). Instead, the inhibitor had a more pronounced effect on the stability of the kinase's beta chain, which is proteolytically processed from the precursor[2]. Thus, it appears that I-OMe-AG538 primarily affects the stability of the kinase rather than its activity in 293T cells. Such a change would not be detected by the chaperone interaction assay.

We did not further investigate BMS-345541, an allosteric IKKα and IKKβ inhibitor. We might have missed it due to the relatively low cellular potency of the inhibitor (IC50 ~4 μM)[3]. In addition, it is known that some allosteric kinase modulators do not increase the thermal stability of the kinase fold[4]. These targets would be missed by our approach.

1. Blum, G., Gazit, A. & Levitzki, A. Substrate competitive inhibitors of IGF-1 receptor kinase. *Biochemistry* **39**, 15705-15712 (2000).
2. Ullrich, A. et al. Insulin-like growth factor I receptor primary structure: comparison with insulin receptor suggests structural determinants that define functional specificity. *Embo J* **5**, 2503-2512 (1986).
3. Burke, J.R. et al. BMS-345541 is a highly selective inhibitor of I kappa B kinase that binds at an allosteric site of the enzyme and blocks NF-kappa B-dependent transcription in mice. *J Biol Chem* **278**, 1450-1456 (2003).
4. Busschots, K. et al. Substrate-Selective Inhibition of Protein Kinase PDK1 by Small Compounds that Bind to the PIF-Pocket Allosteric Docking Site. *Chem Biol* **19**, 1152-1163 (2012).

SUPPLEMENTARY INFORMATION

Supplementary Table 1. List of kinase inhibitors profiled.

Supplementary Table 2. Kinase inhibitor specificities.

Supplementary Table 3. Comparison of EC50 values from the chaperone assay and published or measured GI50 or EC50 values from cellular assays.

Supplementary Figure 1. Chaperone interaction assay measures kinase domain stabilization *in vivo*, not *in vitro*.

(a) 3xFLAG-tagged BCR-ABL was transfected into 293T cells stably expressing the *Renilla*-Hsp90 fusion protein. Cells were either treated with 10 μM inhibitor for 1h before lysis and the LUMIER assay (green bars), or the inhibitors were added directly to the lysate (blue bars). Interaction scores correspond to relative interactions (no inhibitor = 1) +/- SD (n=4). Only ABL1 inhibitors dasatinib, imatinib and ponatinib have an effect on BCR-ABL::HSP90 interaction and only if they are added to the cells prior to lysis. Statistical test for significance was unpaired t-test with unequal variance. ***, $p<0.001$

(b) Experiment was done as in **(a)** but with a 3xFLAG-tagged FLT3 ITD construct. Only the FLT3 inhibitor quizartinib and ponatinib, which also targets FLT3 (ref. [25]), decrease the FLT3-ITD::HSP90 interaction, and only if they are added to the cells prior to lysis. ***, $p<0.001$

Supplementary Figure 2. EC50 values derived from CDC37 and HSP90 interactions are similar.

(a) The effects of imatinib on BCR-ABL::HSP90 and BCR-ABL::CDC37 interactions were measured with LUMIER in triplicate. Imatinib was added to the cells for 1h prior to cell lysis and LUMIER assay. Relative interaction strength (no drug = 1) is plotted against imatinib concentration.

(b) The effects of dasatinib on BCR-ABL::HSP90 and BCR-ABL::CDC37 interactions. Experiment was performed as in **(a)**.

(c) Summary of EC50 values (in nM) derived from **(a)** and **(b)**. 95% confidence intervals are shown in parentheses.

Supplementary Figure 3. Reproducibility of kinase::CDC37 interactions. Kinase::CDC37 interactions were measured with LUMIER with BACON in duplicate on 384-well plates.

Supplementary Figure 4. Examples of EC50 curves from the assay. Examples are shown for strong client proteins ARAF, ETV6-FGFR3 and TFG-NTRK1 (**a**), medium client proteins PIM3, ACVR2B and NEK11 (**b**), and weak client proteins AKT2, EGFR D770-N771 insNPG and destabilized MAP2K1 (I172A/I175A/L178M). Calculated EC50 values are indicated. Error bars indicate standard deviation.

Supplementary Figure 5. Comparison of kinase targets identified by chaperone interaction assay and KINOMEscan technology.

Venn diagram of kinase inhibitor targets that were identified in inhibitor profiling assays and that were tested by both assays (chaperone assay, blue; KINOMEscan[5], yellow). Statistical significance of the overlap was tested with Fisher's exact test. Blue numbers correspond to kinase targets that were identified by the chaperone assay but were not in the *in vitro* panel. Orange numbers correspond to kinase targets that were identified *in vitro* but were not in the chaperone assay kinase panel. For *in vitro* hits, targets with IC50 at or below 1000 nM were considered.

Supplementary Figure 6. Analysis of discordant results between the chaperone assay and *in vitro* binding assay.

(a) Results from the chaperone assay correlate well with in vivo inhibitor activity. Six kinases that were identified as staurosporine targets *in vitro* but did not score in our assay were transfected into 293T cells and assayed for autophosphorylation after 1h staurosporine treatment. In four cases, staurosporine did not markedly decrease phosphotyrosine content of the kinase, consistent with the primary screen results. In one case (FER), staurosporine did inhibit the kinase, but in a repeated LUMIER assay, the kinase proved to be a target of the inhibitor. One kinase, FLT4, did not dissociate from Hsp90 although its phosphotyrosine content was affected by staurosporine treatment. Previously reported IC50 values from *in vitro* KINOMEscan assay are shown.

(b) JAK1 was not reported to be a staurosporine target *in vitro* but was identified in the chaperone screen. JAK1 was transfected into 293T cells, which were treated with staurosporine for 1h. Treatment led to markedly reduced pTyr content of the kinase, consistent with JAK1 being a staurosporine target *in vivo*.

Supplementary Figure 7. Correlation between EC50 values derived from the chaperone assay with measured or previously reported cellular potencies.

Compound potencies were measured with the chaperone assay (**Supplementary Table 2**), and cellular potencies (GI50 or EC50) were collected through a comprehensive literature search. Only assays in which the cellular potency could be unequivocally linked to a specific drug/target interaction were included in the analysis. Drug/target pairs are indicated. For each pair, data for multiple mutant variants were included, if available. Primary data is available in **Supplementary Table 3**.

Supplementary Figure 8. Allosteric kinase inhibitors have very few if any off-targets.

(a-c) 293T cells stably expressing CDC37-*Renilla* luciferase fusion protein and transfected with 3xFLAG tagged kinases were treated with 5 μM MK2206 (**a**), Kin001-102 (**b**) or trametinib (**c**) or vehicle in duplicate for 1 hour prior to the LUMIER assay. Known drug targets that were profiled by the assay are indicated as colored circles.

Supplementary Figure 9. GNF-2 is a highly selective allosteric ABL1 and BCR-ABL inhibitor.

(a) Chaperone interaction profiling identifies only ABL1, BCR-ABL and their variants as GNF-2 targets. However, one BCR-ABL variant, P439T/I502M (green circle) was not affected by the GNF-2 treatment. BCR-ABL variants that were identified as GNF-2 resistant in an earlier study[16] are shown as blue circles, native BCR-ABL as a whithe circle.

(b) The effect of GNF-2 on the interaction of HSP90 with BCR-ABL variants is an indicator of GNF-2 resistance. BCR-ABL variants were rank-ordered based on the relative change in HSP90 interaction upon GNF-2 treatment **(a)**. Blue bars indicate variants that were recovered in an independent cellular screen for GNF-2 resistant variants[16]. Horizontal line indicates the change in interaction between HSP90 and native BCR-ABL. Statistical significance was tested with Wilcoxon rank sum test.

(c) P439T/I502M variant is less sensitive to GNF-2 in a cellular growth assay. Ba/F3 cells were transformed with a retrovirus expressing native BCR-ABL or the P493T/I502M variant. Cell viability was measured after treating the cells with GNF-2.

Supplementary Figure 10. Secondary crizotinib targets. Indicated kinases were transfected into *Renilla*-Hsp90 cells (for EC50 values) or 293T cells (western blotting), and the cells were treated with increasing concentrations of crizotinib for 1 hour. Inhibitor EC50 values were measured with LUMIER assay (top). Error bars indicate standard deviation. For phosphotyrosine blotting (bottom), kinases were immunoprecipitated with anti-FLAG antibody, and kinase autophosphorylation was assessed with anti-phosphotyrosine antibody. The efficiency of immunoprecipitation was measured with an anti-FLAG antibody. Asterisk denotes a non-specific pTyr-containing protein in ABL1 immunoprecipitation.

Supplementary Figure 11. Secondary cell line M091-TA established from M091 cells remains highly sensitive to crizotinib.

M091-TA cell line was established from a surgically removed M091 xenograft tumor. Sensitivity to 48-hour treatment with crizotinib was measured with alamarBlue assay in triplicate. Error bars indicate standard deviation (n=3).

Supplementary Figure 12.

Immunohistochemical analysis of crizotinib-treated tumor xenografts. Crizotinib-treated tumors and control tumors were surgically removed from mice and immunohistochemically stained for proliferation marker phospho-histone H3S10 (left panel) or for total phosphotyrosine content (right panel).

Supplementary Figure 13. Analysis of false positives from the primary screen.

(a-b) The primary target of HG-6-64-1, EPHA2, was not identified in the primary screen. However, re-testing the kinase by LUMIER assay (**a**) and by western blotting (**b**) after HG-6-64-1 treatment confirmed it as a target.

(c-d) One of the primary targets of afatinib, EGFR L858R, was not identified in the primary screen. Re-testing the kinase by LUMIER assay (**c**) and by western blotting (**d**) after 1-hour afatinib treatment confirmed it as a target.

(e) The primary target of I-OMe-AG538 is IGF1R. It was not identified in the chaperone screen. IGF1R was transfected into 293T cells and the cells were treated with increasing concentrations of I-OMe-AG538. The inhibitor has a more pronounced effect on the levels of the processed, catalytic beta chain (left panel) than on its phosphotyrosine content (right panel).

Supplementary Figure 1

A

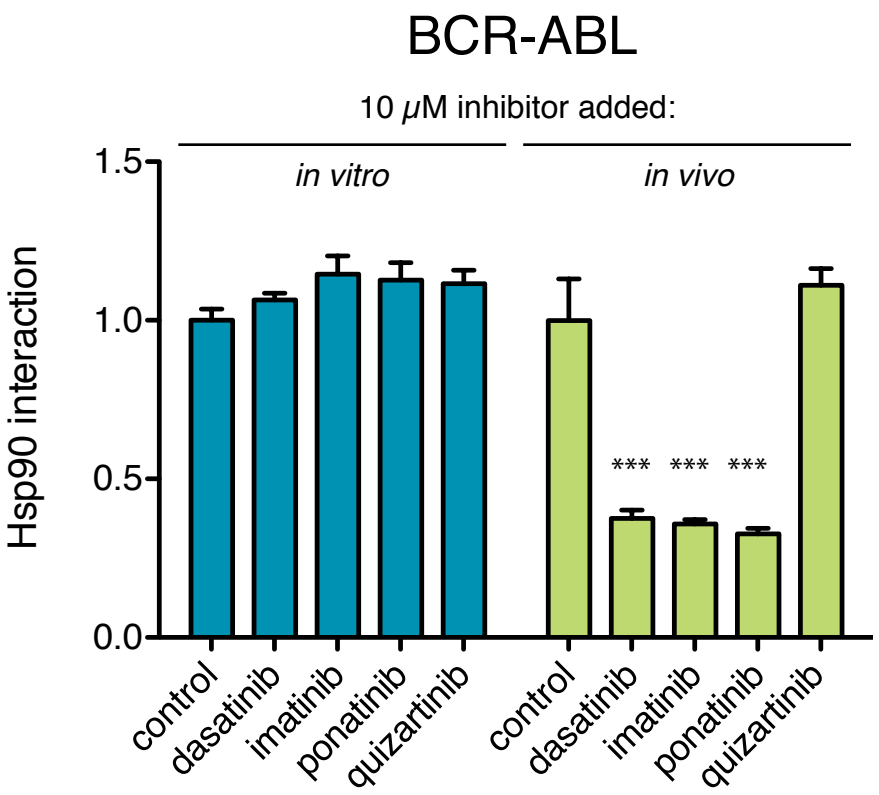

B

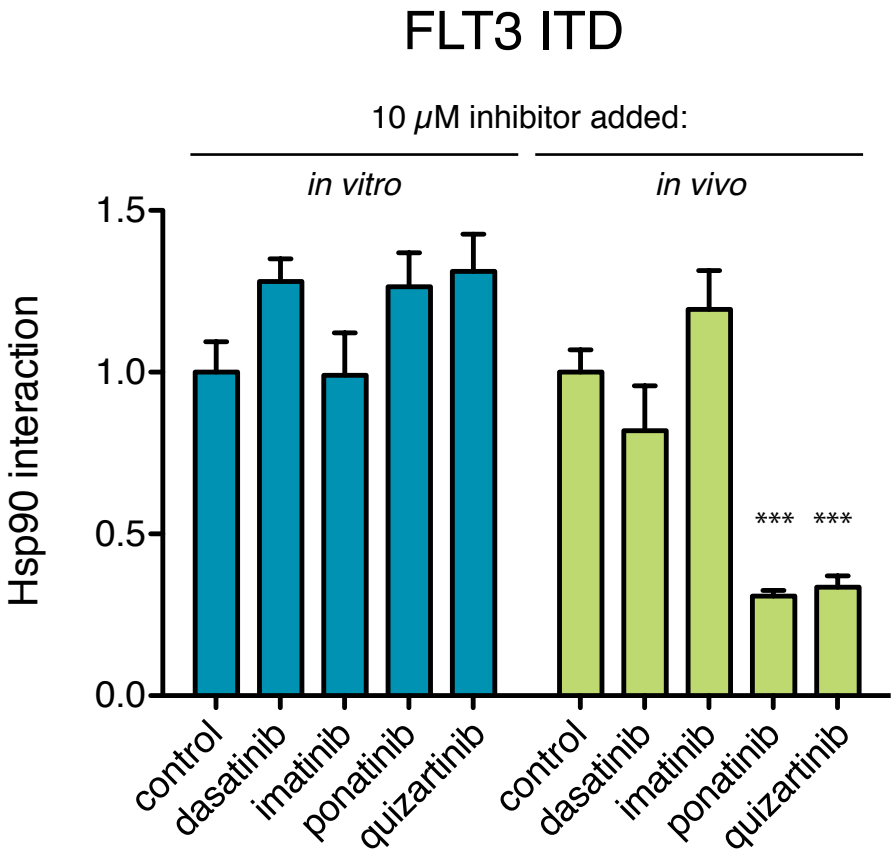

Supplementary Figure 2

A

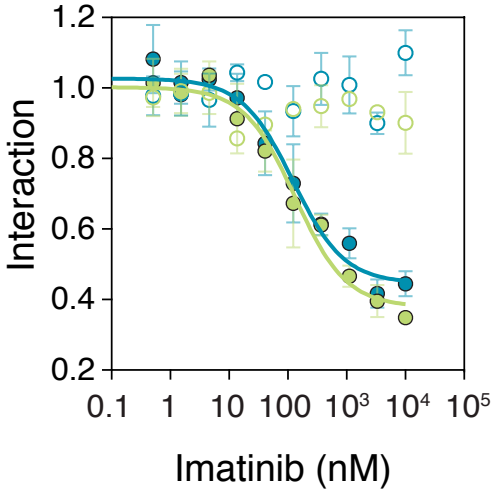

B

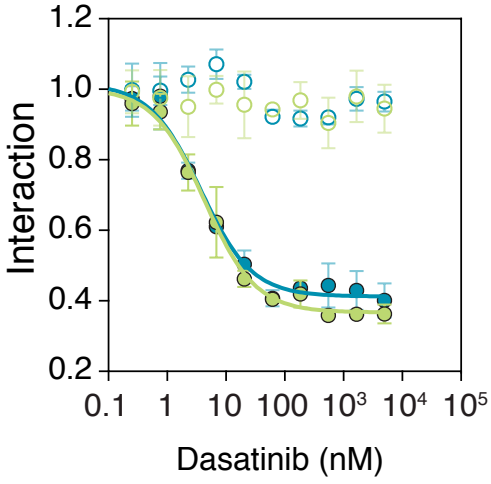

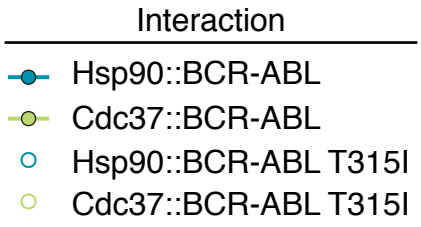

C

Inhibitor	**Sensor**	
	Hsp90	Cdc37
Imatinib	123 (75-201)	133 (86-204)
Dasatinib	4 (2-5)	4 (3-6)

Supplementary Figure 3

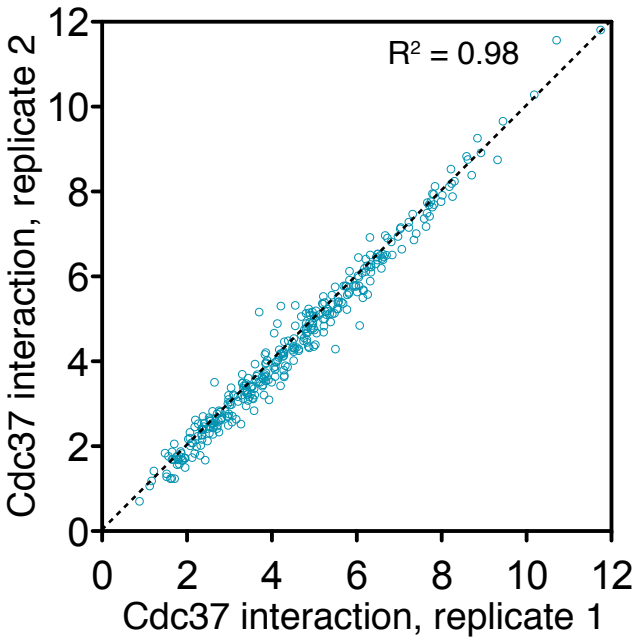

Supplementary Figure 4

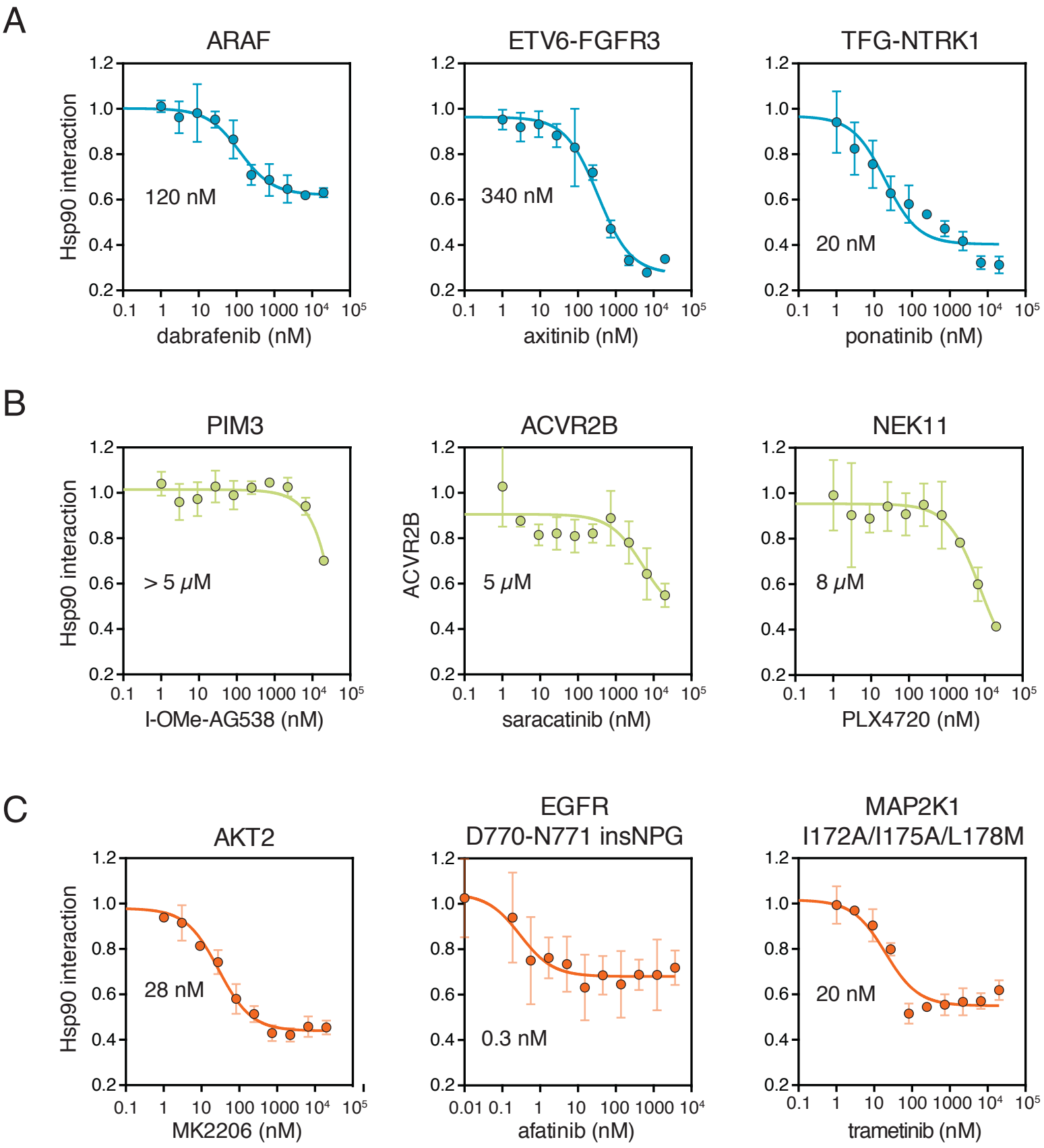

Supplementary Figure 5

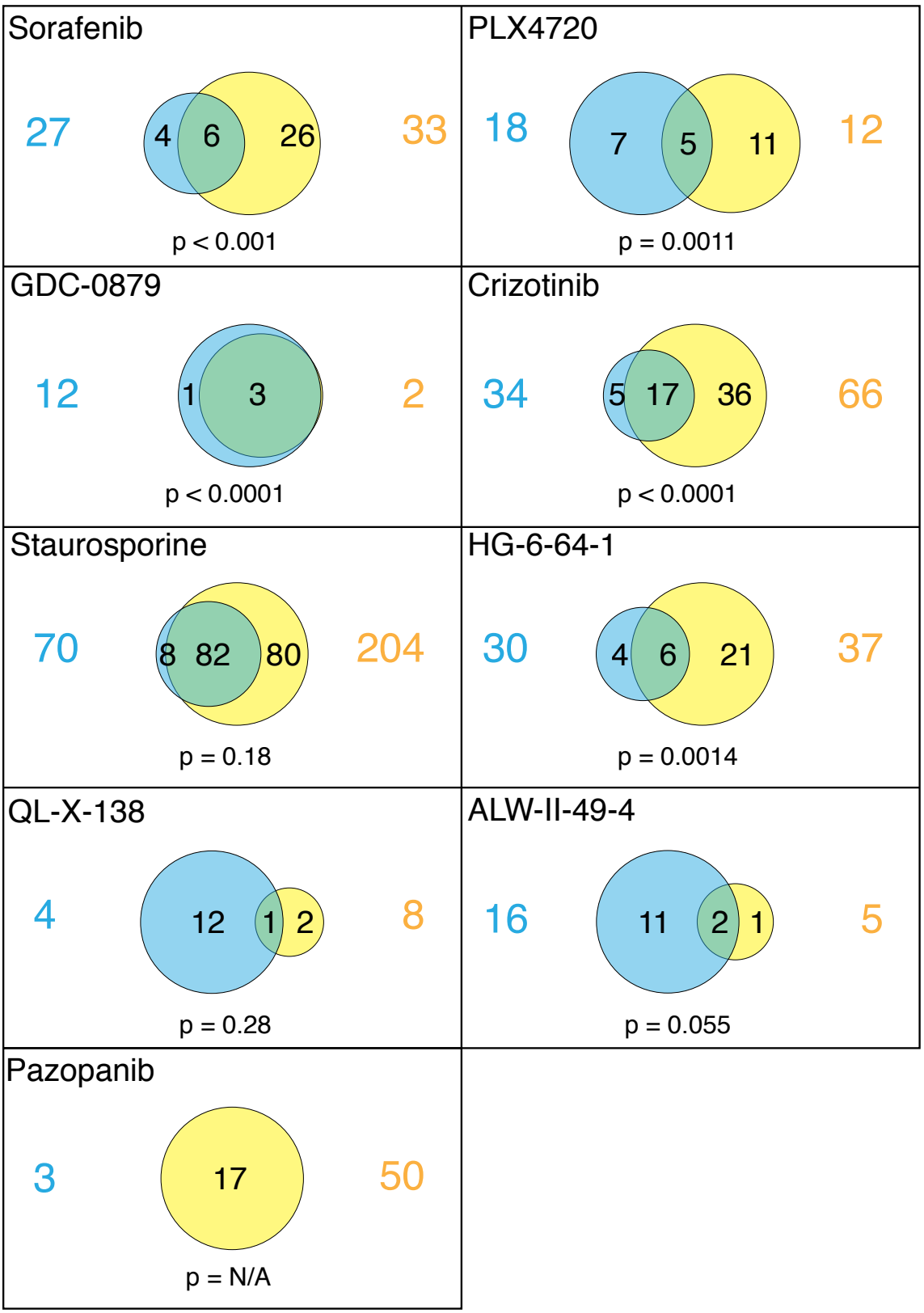

Supplementary Figure 6

A

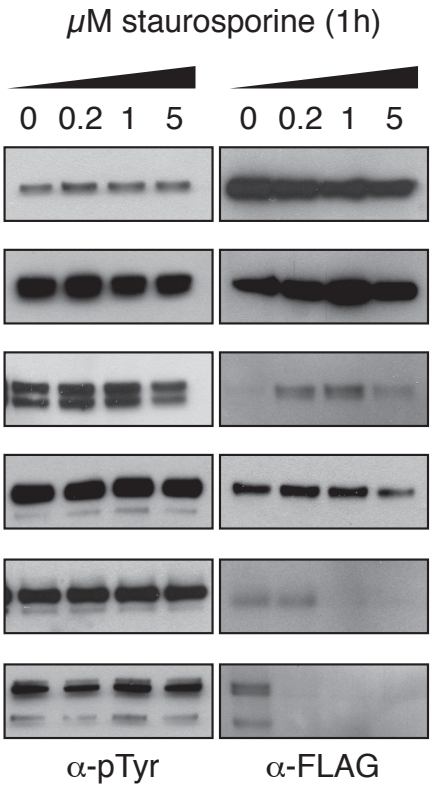

kinase	IC50 (nM) KINOMEscan	EC50 (nM) this study	class
YES1	52	N/A	true negative
DDR1	19	N/A	true negative
DDR2	42	N/A	true negative
EPHB1	240	N/A	true negative
FER	24	410	false negative in primary assay
FLT4	28	N/A	false negative?

B

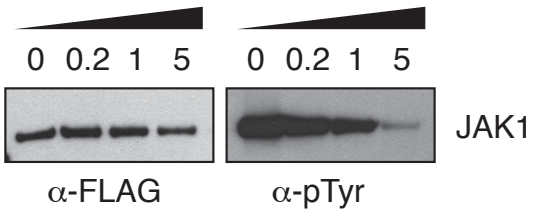

Supplementary Figure 7

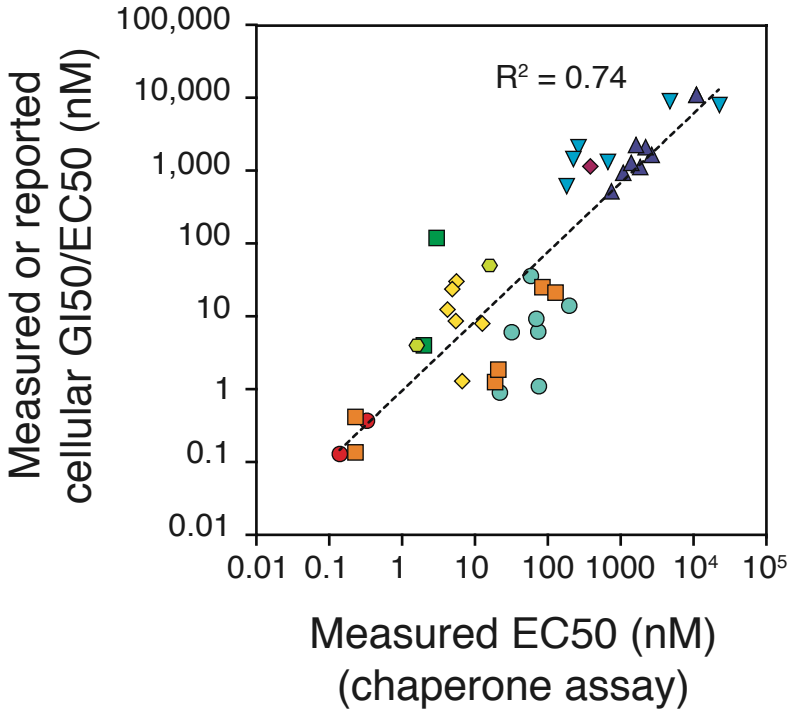

target(s)	compound(s)
AR,GR	steroid hormones
FLT3 ITD	quizartinib
BCR-ABL	dasatinib
PDGFR	sorafenib
EGFR	afatinib
BCR-ABL	ponatinib
BCR-ABL	imatinib
BCR-ABL	GNF-2
BCR-ABL	DPH

Supplementary Figure 8

A

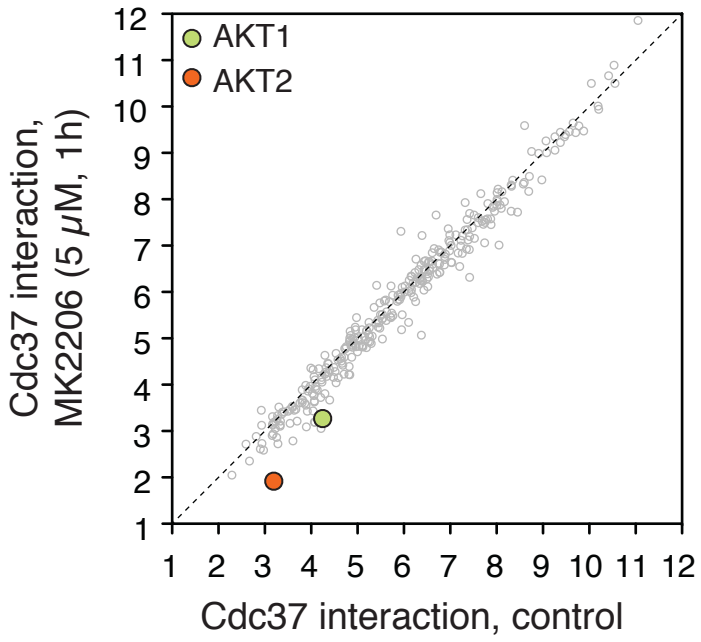

B

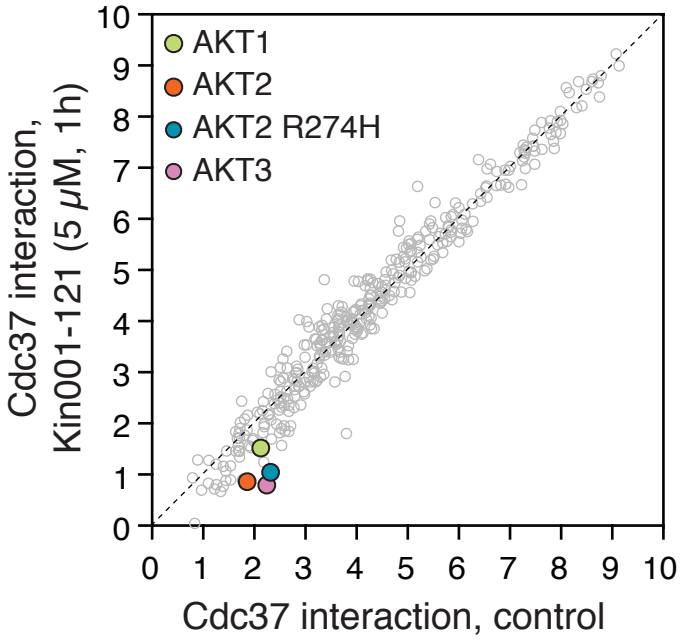

C

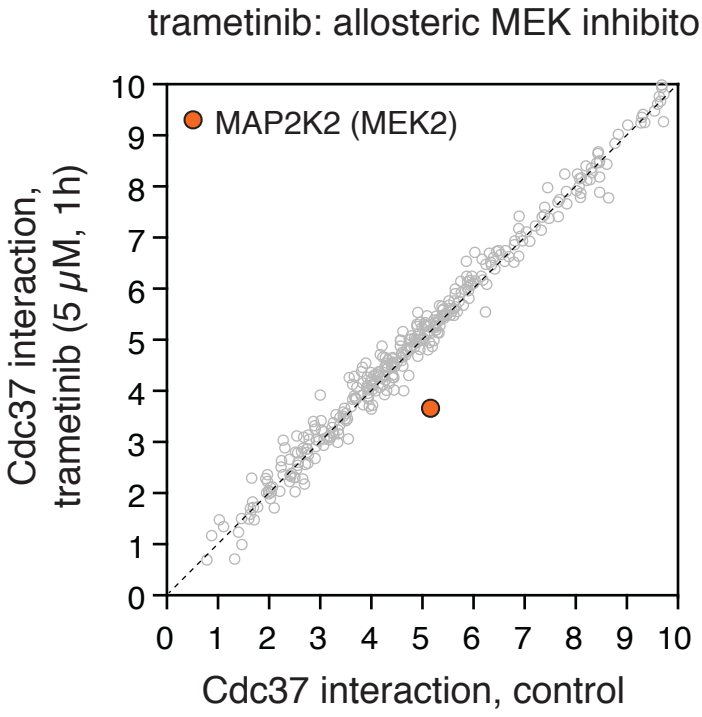

Supplementary Figure 9

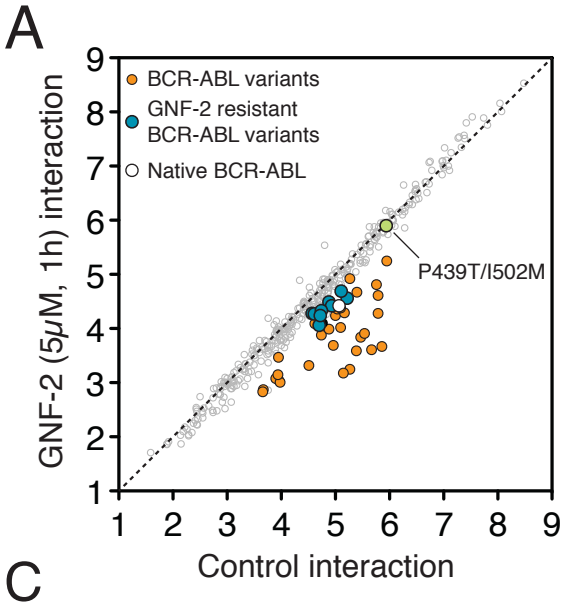

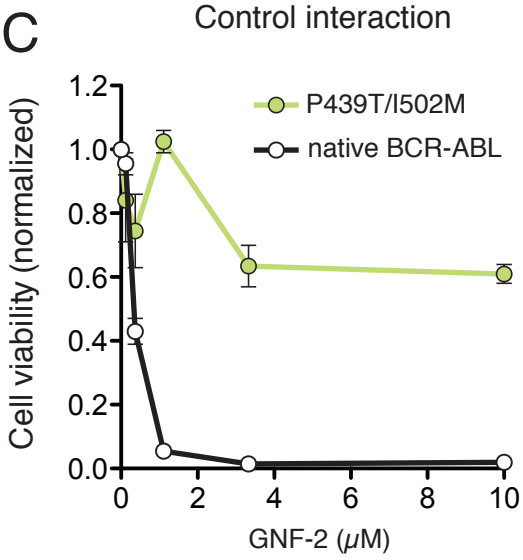

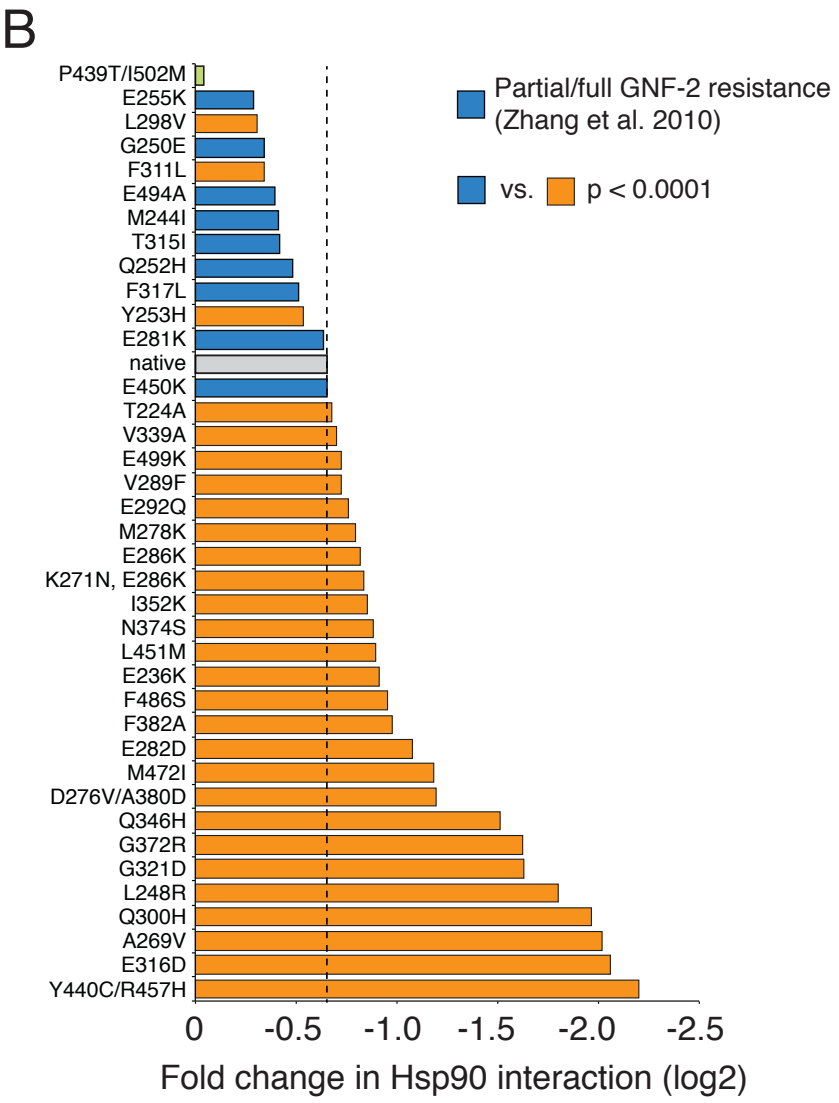

Supplementary Figure 10

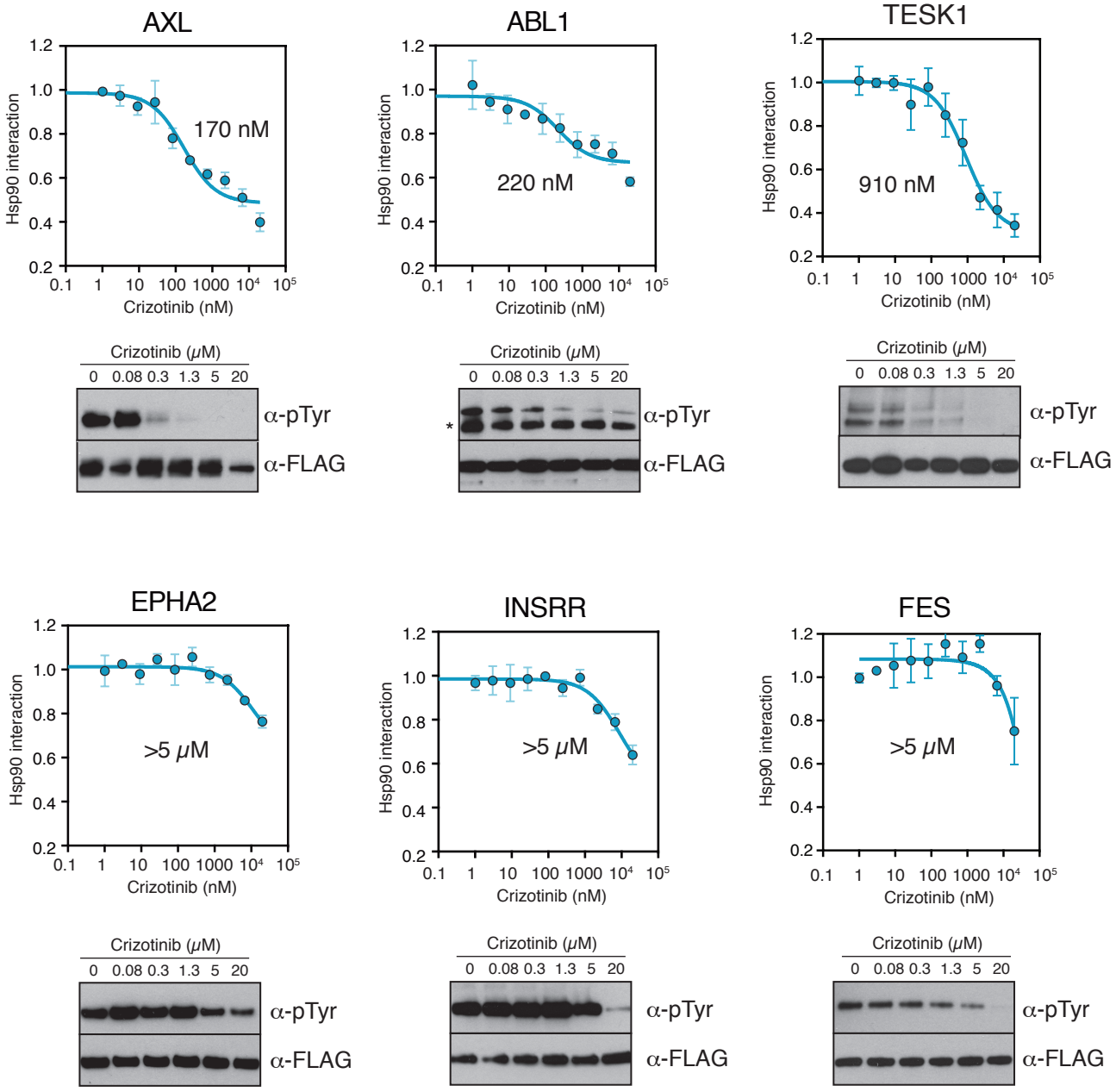

Supplementary Figure 11

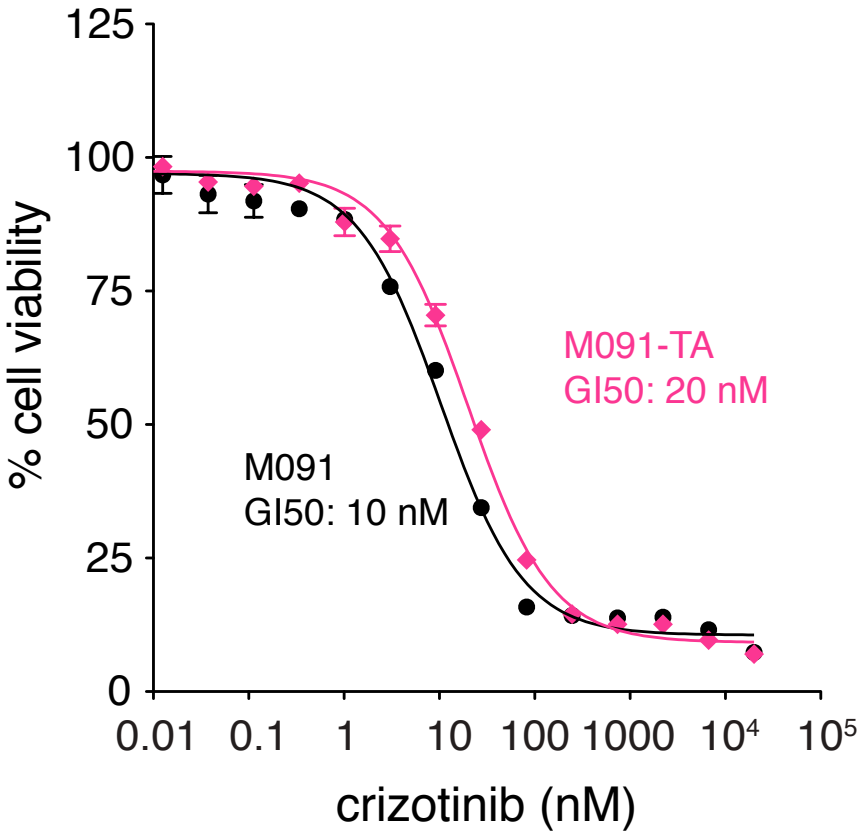

Supplementary Figure 12

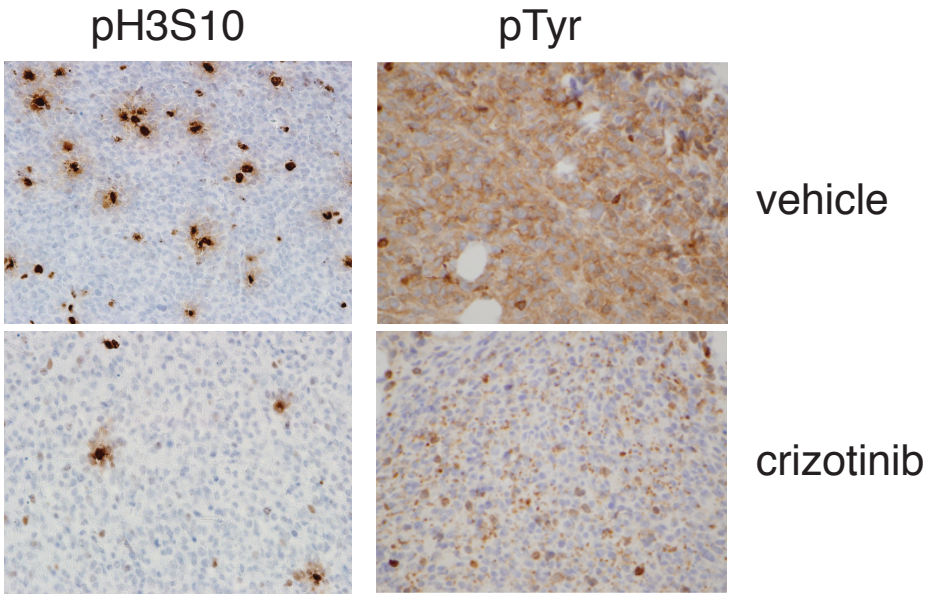

Supplementary Figure 13

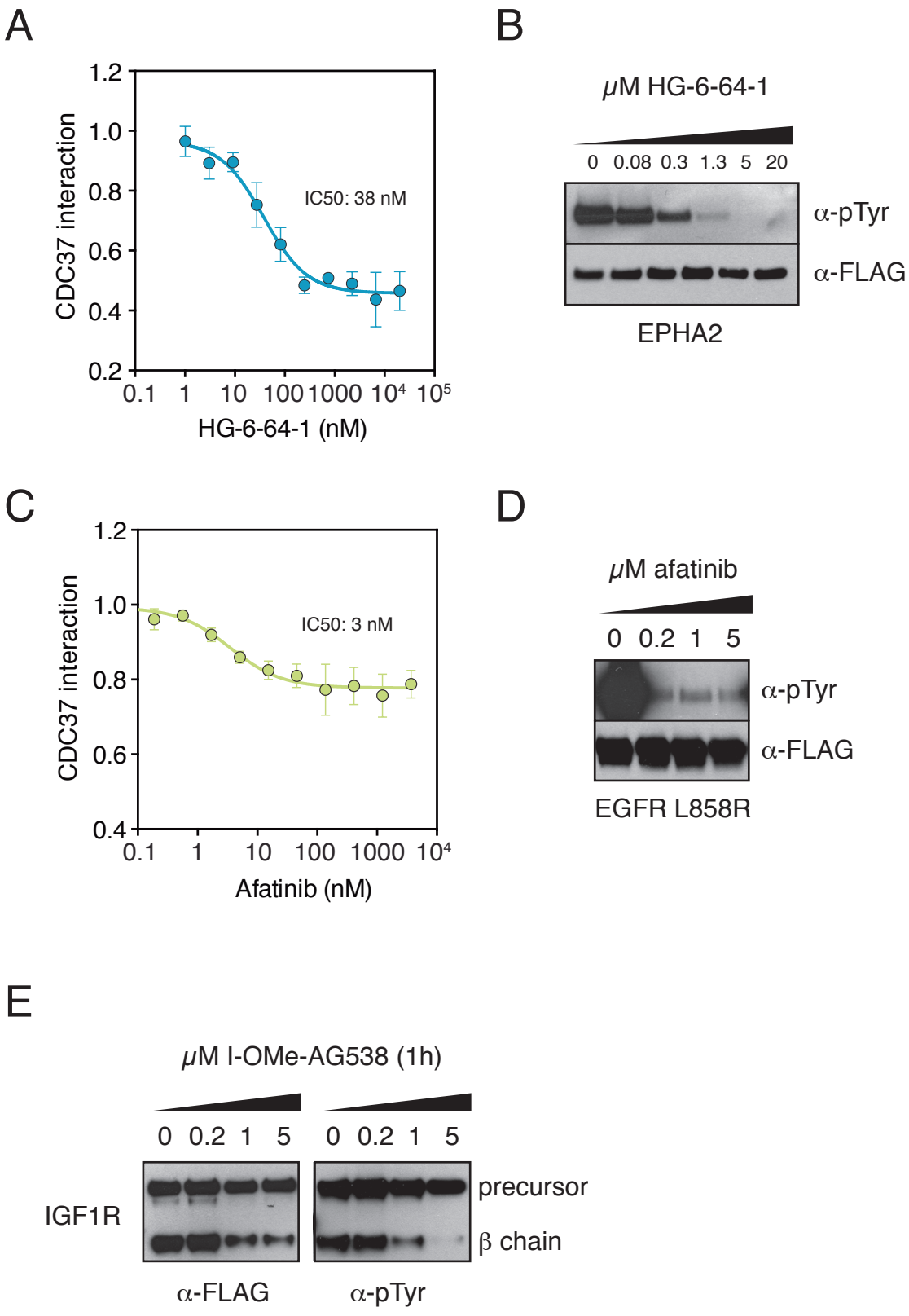

Supplementary Table 1. List of kinase inhibitors.

Inhibitor	Name	CAS	Type	In clinical trials?	Primary target	Primary target found in the primary screen?	Profiled with Hsp90 or Cdc37?
AG-013736	axitinib/Inlyta	319460-85-0	ATP-competitive	FDA-approved	VEGFR, PDGFR	yes (PDGFR)	Cdc37
ALW-II-38-3		N/A	ATP-competitive		EPHB2	no (EPHB2 not in the collection)	Cdc37
ALW-II-49-7		N/A	ATP-competitive		EPHB2	no (EPHB2 not in the collection)	Cdc37
AP24534	ponatinib	943319-70-8	ATP-competitive	Submitted for FDA approval	BCR-ABL (T315I)	yes	Cdc37
AZD0530	saracatinib	379231-04-6	ATP-competitive	Phase II	SRC/ABL	yes	Cdc37
BAY 43-9006	sorafenib/Nexavar	284461-73-0	ATP-competitive	FDA-approved	BRAF/tyrosine kinases	yes	Cdc37
BIBW2992	afatinib/Tomtovok	439081-18-2	irreversible	Phase III	EGFR	no	Cdc37
BAY 73-4506	regorafenib/Stivarga	755037-03-7	ATP-competitive	FDA-approved	VEGFR, PDGFR, KIT, RET, RAF	yes (FIP1L1-PDGFRA, ETV6-PDGFRA)	Cdc37
BMS-345541		547757-23-3	allosteric		IKBKB	no	Cdc37
DPH		484049-04-9	allosteric (activator)		ABL/BCR-ABL	yes	Cdc37
GDC-0879		905281-76-7	ATP-competitive		BRAF	yes	Cdc37
GNF-2		778270-11-4	allosteric		ABL/BCR-ABL	yes	Hsp90
HG-6-64-1		N/A	ATP-competitive		EPHA2	no	Cdc37
GSK1120212	trametinib	871700-17-3	allosteric	Submitted for FDA approval	MEK1/MEK2	yes (MEK2)	Cdc37
KIN001-102		N/A	allosteric		AKT	yes (AKT1, AKT2)	Cdc37
GSK2118436A	dabrafenib	1195765-45-7	ATP-competitive	Submitted for FDA approval	BRAF	yes (BRAF)	Cdc37
MK2206		1032350-13-2	allosteric	Phase II	AKT	yes (AKT1, AKT2)	Cdc37
GW786034	pazopanib/Votrient	444731-52-6	ATP-competitive	FDA-approved	VEGFR, PDGFR	no	Cdc37
PLX4032	vemurafenib/Zelboraf	918504-65-1	ATP-competitive	FDA-approved	BRAF (V600E)	yes (BRAF)	Hsp90
I-OMe-AG 538		N/A	allosteric		IGF1R	no	Cdc37
PLX4720		918505-84-7	ATP-competitive		BRAF (V600E)	yes (BRAF)	Cdc37
LRRK2-IN-1		1234480-84-2	ATP-competitive		LRRK2	no (LRRK2 does not bind Cdc37)	Cdc37
QL-X-138		N/A	irreversible		BTK, MNK2, MTOR	yes (BTK)	Cdc37
PF-02341066	crizotinib/Xalkori	877399-52-5	ATP-competitive	FDA-approved	ALK/MET	yes (ALK R1275Q)	Hsp90
R788	fostamatinib	901119-35-5	ATP-competitive	Phase III	SYK	yes (SYK, ETV6-SYK)	Cdc37
staurosporine		62996-74-1	ATP-competitive		pan-kinase inhibitor	N/A	Hsp90
WZ3105		N/A	irreversible		CLK2, CSNK1E, FLT3, ULK1	yes (ETV6-FLT3)	Cdc37
ThZ-2-98-1		N/A	irreversible		IRAK1	no (IRAK1 not tested)	Cdc37
XL184	cabozantinib	849217-68-1	ATP-competitive	Submitted for FDA approval	MET, VEGFR2	no (MET does not bind Cdc37, VEGFR2 not tested)	Cdc37
Torin1		1222998-36-8	ATP-competitive		MTOR	no (mTOR does not bind Cdc37)	Cdc37